

## First Measurement of the Branching Ratio of $J/\psi \rightarrow \gamma f_2(1270) f_2(1270)$

M. Ablikim<sup>1</sup>, J. Z. Bai<sup>1</sup>, Y. Ban<sup>10</sup>, J. G. Bian<sup>1</sup>, X. Cai<sup>1</sup>, J. F. Chang<sup>1</sup>, H. F. Chen<sup>16</sup>, H. S. Chen<sup>1</sup>, H. X. Chen<sup>1</sup>, J. C. Chen<sup>1</sup>, Jin Chen<sup>1</sup>, Jun Chen<sup>6</sup>, M. L. Chen<sup>1</sup>, Y. B. Chen<sup>1</sup>, S. P. Chi<sup>2</sup>, Y. P. Chu<sup>1</sup>, X. Z. Cui<sup>1</sup>, H. L. Dai<sup>1</sup>, Y. S. Dai<sup>18</sup>, Z. Y. Deng<sup>1</sup>, L. Y. Dong<sup>1</sup>, S. X. Du<sup>1</sup>, Z. Z. Du<sup>1</sup>, J. Fang<sup>1</sup>, S. S. Fang<sup>2</sup>, C. D. Fu<sup>1</sup>, H. Y. Fu<sup>1</sup>, C. S. Gao<sup>1</sup>, Y. N. Gao<sup>14</sup>, M. Y. Gong<sup>1</sup>, W. X. Gong<sup>1</sup>, S. D. Gu<sup>1</sup>, Y. N. Guo<sup>1</sup>, Y. Q. Guo<sup>1</sup>, Z. J. Guo<sup>15</sup>, F. A. Harris<sup>15</sup>, K. L. He<sup>1</sup>, M. He<sup>11</sup>, X. He<sup>1</sup>, Y. K. Heng<sup>1</sup>, H. M. Hu<sup>1</sup>, T. Hu<sup>1</sup>, G. S. Huang<sup>1†</sup>, L. Huang<sup>6</sup>, X. P. Huang<sup>1</sup>, X. B. Ji<sup>1</sup>, Q. Y. Jia<sup>10</sup>, C. H. Jiang<sup>1</sup>, X. S. Jiang<sup>1</sup>, D. P. Jin<sup>1</sup>, S. Jin<sup>1</sup>, Y. Jin<sup>1</sup>, Y. F. Lai<sup>1</sup>, F. Li<sup>1</sup>, G. Li<sup>1</sup>, H. H. Li<sup>1</sup>, J. Li<sup>1</sup>, J. C. Li<sup>1</sup>, Q. J. Li<sup>1</sup>, R. B. Li<sup>1</sup>, R. Y. Li<sup>1</sup>, S. M. Li<sup>1</sup>, W. G. Li<sup>1</sup>, X. L. Li<sup>7</sup>, X. Q. Li<sup>9</sup>, X. S. Li<sup>14</sup>, Y. F. Liang<sup>13</sup>, H. B. Liao<sup>5</sup>, C. X. Liu<sup>1</sup>, F. Liu<sup>5</sup>, Fang Liu<sup>16</sup>, H. M. Liu<sup>1</sup>, J. B. Liu<sup>1</sup>, J. P. Liu<sup>17</sup>, R. G. Liu<sup>1</sup>, Z. A. Liu<sup>1</sup>, Z. X. Liu<sup>1</sup>, F. Lu<sup>1</sup>, G. R. Lu<sup>4</sup>, J. G. Lu<sup>1</sup>, C. L. Luo<sup>8</sup>, X. L. Luo<sup>1</sup>, F. C. Ma<sup>7</sup>, J. M. Ma<sup>1</sup>, L. L. Ma<sup>11</sup>, Q. M. Ma<sup>1</sup>, X. Y. Ma<sup>1</sup>, Z. P. Mao<sup>1</sup>, X. H. Mo<sup>1</sup>, J. Nie<sup>1</sup>, Z. D. Nie<sup>1</sup>, S. L. Olsen<sup>15</sup>, H. P. Peng<sup>16</sup>, N. D. Qi<sup>1</sup>, C. D. Qian<sup>12</sup>, H. Qin<sup>8</sup>, J. F. Qiu<sup>1</sup>, Z. Y. Ren<sup>1</sup>, G. Rong<sup>1</sup>, L. Y. Shan<sup>1</sup>, L. Shang<sup>1</sup>, D. L. Shen<sup>1</sup>, X. Y. Shen<sup>1</sup>, H. Y. Sheng<sup>1</sup>, F. Shi<sup>1</sup>, X. Shi<sup>10</sup>, H. S. Sun<sup>1</sup>, S. S. Sun<sup>16</sup>, Y. Z. Sun<sup>1</sup>, Z. J. Sun<sup>1</sup>, X. Tang<sup>1</sup>, N. Tao<sup>16</sup>, Y. R. Tian<sup>14</sup>, G. L. Tong<sup>1</sup>, G. S. Varner<sup>15</sup>, D. Y. Wang<sup>1</sup>, J. Z. Wang<sup>1</sup>, K. Wang<sup>16</sup>, L. Wang<sup>1</sup>, L. S. Wang<sup>1</sup>, M. Wang<sup>1</sup>, P. Wang<sup>1</sup>, P. L. Wang<sup>1</sup>, S. Z. Wang<sup>1</sup>, W. F. Wang<sup>1</sup>, Y. F. Wang<sup>1</sup>, Zhe Wang<sup>1</sup>, Z. Wang<sup>1</sup>, Zheng Wang<sup>1</sup>, Z. Y. Wang<sup>1</sup>, C. L. Wei<sup>1</sup>, D. H. Wei<sup>3</sup>, N. Wu<sup>1</sup>, Y. M. Wu<sup>1</sup>, X. M. Xia<sup>1</sup>, X. X. Xie<sup>1</sup>, B. Xin<sup>7</sup>, G. F. Xu<sup>1</sup>, H. Xu<sup>1</sup>, Y. Xu<sup>1</sup>, S. T. Xue<sup>1</sup>, M. L. Yan<sup>16</sup>, F. Yang<sup>9</sup>, H. X. Yang<sup>1</sup>, J. Yang<sup>16</sup>, S. D. Yang<sup>1</sup>, Y. X. Yang<sup>3</sup>, M. Ye<sup>1</sup>, M. H. Ye<sup>2</sup>, Y. X. Ye<sup>16</sup>, L. H. Yi<sup>6</sup>, Z. Y. Yi<sup>1</sup>, C. S. Yu<sup>1</sup>, G. W. Yu<sup>1</sup>, C. Z. Yuan<sup>1</sup>, J. M. Yuan<sup>1</sup>, Y. Yuan<sup>1</sup>, Q. Yue<sup>1</sup>, S. L. Zang<sup>1</sup>, Yu. Zeng<sup>1</sup>, Y. Zeng<sup>6</sup>, B. X. Zhang<sup>1</sup>, B. Y. Zhang<sup>1</sup>, C. C. Zhang<sup>1</sup>, D. H. Zhang<sup>1</sup>, H. Y. Zhang<sup>1</sup>, J. Zhang<sup>1</sup>, J. Y. Zhang<sup>1</sup>, J. W. Zhang<sup>1</sup>, L. S. Zhang<sup>1</sup>, Q. J. Zhang<sup>1</sup>, S. Q. Zhang<sup>1</sup>, X. M. Zhang<sup>1</sup>, X. Y. Zhang<sup>11</sup>, Y. J. Zhang<sup>10</sup>, Y. Y. Zhang<sup>1</sup>, Yiyun Zhang<sup>13</sup>, Z. P. Zhang<sup>16</sup>, Z. Q. Zhang<sup>4</sup>, D. X. Zhao<sup>1</sup>, J. B. Zhao<sup>1</sup>, J. W. Zhao<sup>1</sup>, M. G. Zhao<sup>9</sup>, P. P. Zhao<sup>1</sup>, W. R. Zhao<sup>1</sup>, X. J. Zhao<sup>1</sup>, Y. B. Zhao<sup>1</sup>, Z. G. Zhao<sup>1\*</sup>, H. Q. Zheng<sup>10</sup>, J. P. Zheng<sup>1</sup>, L. S. Zheng<sup>1</sup>, Z. P. Zheng<sup>1</sup>, X. C. Zhong<sup>1</sup>, B. Q. Zhou<sup>1</sup>, G. M. Zhou<sup>1</sup>, L. Zhou<sup>1</sup>, N. F. Zhou<sup>1</sup>, K. J. Zhu<sup>1</sup>, Q. M. Zhu<sup>1</sup>, Y. C. Zhu<sup>1</sup>, Y. S. Zhu<sup>1</sup>, Yingchun Zhu<sup>1</sup>, Z. A. Zhu<sup>1</sup>, B. A. Zhuang<sup>1</sup>, B. S. Zou<sup>1</sup>.

(BES Collaboration)

<sup>1</sup> Institute of High Energy Physics, Beijing 100039, People's Republic of China

<sup>2</sup> China Center of Advanced Science and Technology, Beijing 100080, People's Republic of China

<sup>3</sup> Guangxi Normal University, Guilin 541004, People's Republic of China

<sup>4</sup> Henan Normal University, Xinxiang 453002, People's Republic of China

<sup>5</sup> Huazhong Normal University, Wuhan 430079, People's Republic of China

<sup>6</sup> Hunan University, Changsha 410082, People's Republic of China

<sup>7</sup> Liaoning University, Shenyang 110036, People's Republic of China

<sup>8</sup> Nanjing Normal University, Nanjing 210097, People's Republic of China

<sup>9</sup> Nankai University, Tianjin 300071, People's Republic of China

<sup>10</sup> Peking University, Beijing 100871, People's Republic of China

<sup>11</sup> Shandong University, Jinan 250100, People's Republic of China

<sup>12</sup> Shanghai Jiaotong University, Shanghai 200030, People's Republic of China

<sup>13</sup> Sichuan University, Chengdu 610064, People's Republic of China

<sup>14</sup> Tsinghua University, Beijing 100084, People's Republic of China

<sup>15</sup> University of Hawaii, Honolulu, Hawaii 96822, USA

<sup>16</sup> University of Science and Technology of China, Hefei 230026, People's Republic of China

<sup>17</sup> Wuhan University, Wuhan 430072, People's Republic of China

<sup>18</sup> Zhejiang University, Hangzhou 310028, People's Republic of China

\* Visiting professor to University of Michigan, Ann Arbor, MI 48109, USA

† Current address: Purdue University, West Lafayette, Indiana 47907, USA.

Using 58 million  $J/\psi$  events taken with the BESII detector at the Beijing Electron Positron Collider, a new decay mode  $J/\psi \rightarrow \gamma f_2(1270) f_2(1270) \rightarrow \gamma \pi^+ \pi^- \pi^+ \pi^-$  is observed for the first time. The branching ratio is determined to be  $Br(J/\psi \rightarrow \gamma f_2 f_2) = (9.5 \pm 0.7 \pm 1.6) \times 10^{-4}$ , where the quoted errors are statistical and systematic, respectively.

PACS numbers: 13.25.Gv, 14.40.Gx, 13.40.Hq

## I. INTRODUCTION

Precise branching ratios are needed in order to better understand  $J/\psi$  physics. Unfortunately, only about 50 to 60% of  $J/\psi$  decay modes have been observed so far [1]. A sample of 58 million  $J/\psi$  events has been accumulated with the upgraded Beijing Spectrometer (BESII). With this sample, the world's largest, it is possible to systematically study  $J/\psi$  decays.

For the decay  $J/\psi \rightarrow \gamma \pi^+ \pi^- \pi^+ \pi^-$ , studies have been done by MARK III [2, 3], DM2 [4] and BES [5, 6]. A large part of the final state is from  $J/\psi \rightarrow \gamma \rho^0 \rho^0$  [2]. MARK III also reported the observation of  $J/\psi \rightarrow \gamma \eta_c \rightarrow \gamma f_2 f_2 \rightarrow \gamma \pi^+ \pi^- \pi^+ \pi^-$  [3]. In this paper, evidence for the decay  $J/\psi \rightarrow \gamma f_2(1270) f_2(1270) \rightarrow \gamma \pi^+ \pi^- \pi^+ \pi^-$  is observed, and the branching ratio of  $J/\psi \rightarrow \gamma f_2(1270) f_2(1270)$  is measured for the first time.

## II. BES DETECTOR

BES is a conventional solenoidal magnet detector [7, 8]. A 12-layer vertex chamber (VTC) surrounding the beam pipe provides trigger and trajectory information. A forty-layer main drift chamber (MDC), located radially outside the VTC, provides trajectory and energy loss ( $dE/dx$ ) information for charged tracks over 85% of the total solid angle with a momentum resolution of  $\sigma_p/p = 0.0178\sqrt{1+p^2}$  ( $p$  in GeV/ $c$ ) and a  $dE/dx$  resolution for hadron tracks of  $\sim 8\%$ . An array of 48 scintillation counters surrounding the MDC measures the time-of-flight (TOF) of charged tracks with a resolution of  $\sim 200$  ps for hadrons. Radially outside the TOF system is a 12 radiation length, lead-gas barrel shower counter (BSC). This measures the energies of electrons and photons over  $\sim 80\%$  of the total solid angle with an energy resolution of  $\sigma_E/E = 21\%/\sqrt{E}$  ( $E$  in GeV). Outside the solenoidal coil, which provides a 0.4 Tesla magnetic field over the tracking volume, is an iron flux return that is instrumented with three double layers of proportional counters that identify muons of momentum greater than 0.5 GeV/ $c$ .

A Geant3 based Monte Carlo, SIMBES, which simulates the detector response, including interactions of secondary particles in the detector material, is used in this analysis. Reasonable agreement between data and Monte Carlo simulation is observed in various channels tested, including  $e^+e^- \rightarrow (\gamma)e^+e^-$ ,  $e^+e^- \rightarrow (\gamma)\mu\mu$ ,  $J/\psi \rightarrow p\bar{p}$ ,  $J/\psi \rightarrow \rho\pi$  and  $\psi(2S) \rightarrow \pi^+\pi^- J/\psi$ ,  $J/\psi \rightarrow l^+l^-$ .

## III. EVENT SELECTION

First a  $J/\psi \rightarrow \gamma \pi^+ \pi^- \pi^+ \pi^-$  sample is selected. Events are required to have four good charged tracks and one or more photon candidates. A good track, reconstructed from hits in the MDC, must be well fitted to a helix originating from the interaction point; have a polar angle,  $\theta$ , with  $|\cos\theta| < 0.8$ ; and a transverse momentum greater than 60 MeV.

The TOF and  $dE/dx$  information are used for particle identification. To identify pions, we define:

$$\chi_{TOF}(i) = \frac{TOF_{measured} - TOF_{expected-i}}{\sigma_{TOF-i}}$$

$$\chi_{dE/dx}(i) = \frac{PHMP_{measured} - PHMP_{expected-i}}{\sigma_{PHMP-i}}$$

$$Prob(i) = Prob(\chi_{TOF}^2(i) + \chi_{dE/dx}^2(i), 2).$$

Here  $i$  denotes  $\pi$ ,  $K$  and  $p$ . If the charged track has only TOF information or only  $dE/dx$  information, then  $Prob(i)$  is determined using that system only. To identify a pion, it is required that:  $Prob(\pi) > Prob(K)$  and  $Prob(\pi) > Prob(p)$ . At least three tracks must be identified as pions.

To reduce the number of spurious low energy photons produced by secondary hadronic interactions, photon candidates must have a minimum energy of 30 MeV and be outside a cone with a half-angle of  $15^\circ$  around any charged track.

To get higher momentum resolution and to remove backgrounds, events are kinematically fitted to the  $J/\psi \rightarrow \gamma\pi^+\pi^-\pi^+\pi^-$  hypothesis, looping over all photon candidates. The fit with the highest probability is selected, and the  $\chi^2$  of the fit is required to be less than 20.

For  $J/\psi \rightarrow \gamma\pi^+\pi^-\pi^+\pi^-$  decay, a major source of background is from  $J/\psi \rightarrow \pi^0\pi^+\pi^-\pi^+\pi^-$ . To remove events containing a  $\pi^0$  when there are multiple photons,  $|m(\gamma1\gamma2) - m(\pi^0)| > 60$  MeV is required if  $\vec{P}_{miss}$  is in the plane of the two photons,  $\gamma1$  and  $\gamma2$ , i.e.  $|\hat{P}_{miss} \cdot (\hat{r}_{\gamma1} \times \hat{r}_{\gamma2})| < 0.15$ . Here  $\hat{P}_{miss}$  is the unit vector of the missing momentum of all charged tracks;  $\hat{r}_{\gamma1}$  and  $\hat{r}_{\gamma2}$  are unit vectors in the  $\gamma1$  and  $\gamma2$  directions, respectively; and  $m(\gamma1\gamma2)$  is the invariant mass of  $\gamma1$  and  $\gamma2$ . Two additional requirements,  $\chi^2_{\gamma\pi^+\pi^-\pi^+\pi^-} < \chi^2_{\gamma\gamma\pi^+\pi^-\pi^+\pi^-}$  and  $P_{t\gamma}^2 < 0.0015$  GeV<sup>2</sup>, are used to further remove  $J/\psi \rightarrow \pi^0\pi^+\pi^-\pi^+\pi^-$  background.  $P_{t\gamma}$  is the transverse momentum of the  $\pi^+\pi^-\pi^+\pi^-$  system with respect to the photon. Finally, the requirement  $|U_{miss}| = |E_{miss} - P_{miss}| < 0.07$  GeV is used to reject events with multiple photons and charged kaons; here,  $E_{miss}$  and  $P_{miss}$  are, respectively, the missing energy and missing momentum calculated using only the charged particles, which are assumed to be pions.

There are other possible backgrounds such as  $J/\psi \rightarrow \omega\pi^+\pi^-$ ,  $J/\psi \rightarrow \gamma K_s^0 K_s^0$ , and  $J/\psi \rightarrow \gamma K_s^0 K^\pm \pi^\mp$ . The  $J/\psi \rightarrow \omega\pi^+\pi^-$  background is eliminated by the requirement  $|M_{\pi^+\pi^-\pi^0} - M_\omega| > 40$  MeV, where the  $\pi^0$  in  $\pi^0\pi^+\pi^-\pi^+\pi^-$  is associated to the missing momentum and energy determined using only the charged tracks. To remove the  $J/\psi \rightarrow \gamma K_s^0 K_s^0$  background, we require  $|M_{\pi^+\pi^-} - M_{K_s^0}| > 25$  MeV for both  $\pi^+\pi^-$  pairs. To remove the background from  $J/\psi \rightarrow \gamma K_s^0 K^\pm \pi^\mp$ , events are rejected if  $\chi^2(J/\psi \rightarrow \gamma K^\pm \pi^\mp \pi^+\pi^-) < \chi^2(J/\psi \rightarrow \gamma\pi^+\pi^-\pi^+\pi^-)$  when  $|M_{\pi^+\pi^-} - M_{K_s^0}| < 25$  MeV.

Figure 1(a) shows the scatter plot of  $M_{\pi1\pi4}$  versus  $M_{\pi2\pi3}$  for surviving events with  $M_{\pi^+\pi^-\pi^+\pi^-} \geq 2.0$  GeV, where  $\pi1$  ( $\pi3$ ) and  $\pi2$  ( $\pi4$ ) are the  $\pi^+$  and  $\pi^-$  with the higher (lower) momentum. There is a clear signal near  $(M_{\rho^0}, M_{\rho^0})$ . Since according to Monte Carlo study most events from  $J/\psi \rightarrow \gamma f_2 f_2$  have  $\pi^+\pi^-\pi^+\pi^-$  invariant mass greater than 2.6 GeV, the scatter plot of  $M_{\pi1\pi4}$  versus  $M_{\pi2\pi3}$  with  $M_{\pi^+\pi^-\pi^+\pi^-} \geq 2.6$  GeV is shown in Fig. 1(b). An obvious cluster near  $(M_{f_2}, M_{f_2})$  is seen besides the signal near  $(M_{\rho^0}, M_{\rho^0})$ .

There is another possible  $M_{\pi^+\pi^-}$  versus  $M_{\pi^+\pi^-}$  combination, which is  $M_{\pi1\pi2}$  versus  $M_{\pi3\pi4}$ . Monte Carlo studies of  $J/\psi \rightarrow \gamma f_2 f_2$  and  $J/\psi \rightarrow \gamma \rho^0 \rho^0$  show that the  $f_2 f_2$  and  $\rho^0 \rho^0$  signal almost always appears in the  $M_{\pi1\pi4}$  versus  $M_{\pi2\pi3}$  combination. Therefore we use the  $M_{\pi1\pi4}$  versus  $M_{\pi2\pi3}$  combination to study  $J/\psi \rightarrow \gamma f_2 f_2$  decay. The  $M_{\pi1\pi4}$  and  $M_{\pi2\pi3}$  distributions for  $M_{\pi^+\pi^-\pi^+\pi^-} \geq 2.6$  GeV are shown in Fig. 1(c) and Fig. 1(d) respectively. Besides the  $\rho$  peak, a peak near  $M_{f_2}$  (1.275 GeV) can be clearly seen in both of these plots.

#### IV. BACKGROUND ANALYSIS

Possible backgrounds are studied using simulated exclusive channels normalized according to Particle Data Group (PDG) branching ratios, as well as a 30 million event inclusive  $J/\psi$  decay Monte Carlo sample generated with Lundcharm [9]. Simulated exclusive decays studied are  $J/\psi \rightarrow \gamma \rho^0 \rho^0$ ,  $J/\psi \rightarrow \gamma \pi^+\pi^-\pi^+\pi^-$ ,  $J/\psi \rightarrow \pi^0\pi^+\pi^-\pi^+\pi^-$ ,  $J/\psi \rightarrow \omega\pi^+\pi^-$ ,  $J/\psi \rightarrow \omega f_2 \rightarrow \omega\pi^+\pi^-$ , and  $J/\psi \rightarrow \pi^+\pi^-\pi^+\pi^-$ , where events are generated according to phase space and normalized by PDG [1] branching ratios. After passing the simulated events through our selection criteria, no  $f_2$  signal remains from these channels.

Fig. 2 shows the  $M_{\pi^+\pi^-}$  spectra from data and from 30 million inclusive  $J/\psi$  Monte Carlo decays normalized to 58 million events, where  $M_{\pi^+\pi^-\pi^+\pi^-}$  is required to be greater than 2.6 GeV and the invariant mass of the other  $\pi^+\pi^-$  pair satisfies  $|M_{\pi^+\pi^-} - M_{f_2}| \leq 0.185$  GeV. This  $M_{\pi^+\pi^-}$  spectrum is used to fit the  $J/\psi \rightarrow \gamma f_2 f_2$  signal in Section V. In Fig. 2(a), there is an  $f_2$  signal from  $J/\psi \rightarrow f_2 \rho^\pm \pi^\mp$  decays from the inclusive  $J/\psi$  Monte Carlo sample. After removing this channel, there is no  $f_2$  signal left in the inclusive  $J/\psi$  decay Monte Carlo events, as shown in Fig. 2(b). So the  $f_2$  signal in the  $M_{\pi^+\pi^-}$  spectrum of inclusive

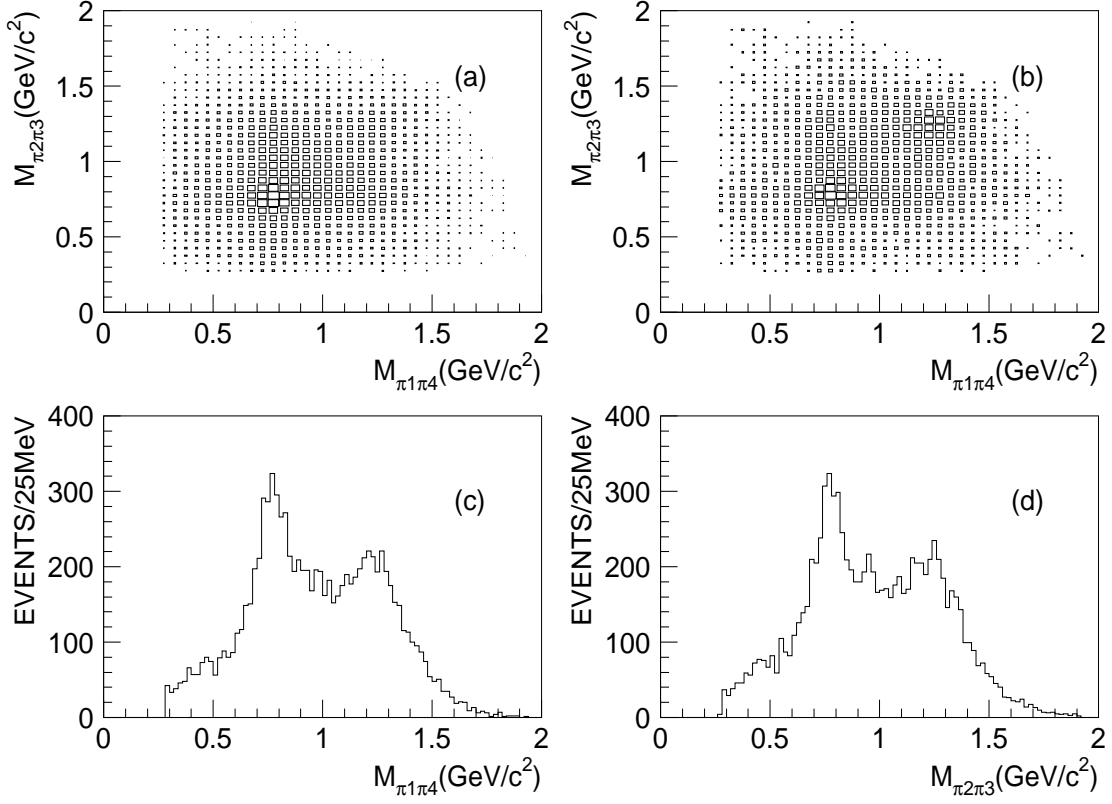


FIG. 1: (a)  $M_{\pi_1\pi_4}$  versus  $M_{\pi_2\pi_3}$  for  $M_{\pi^+\pi^-\pi^+\pi^-} \geq 2.0$  GeV. (b)  $M_{\pi_1\pi_4}$  versus  $M_{\pi_2\pi_3}$  for  $M_{\pi^+\pi^-\pi^+\pi^-} \geq 2.6$  GeV. (c)  $M_{\pi_1\pi_4}$  and (d)  $M_{\pi_2\pi_3}$  distributions with  $M_{\pi^+\pi^-\pi^+\pi^-} \geq 2.6$  GeV.

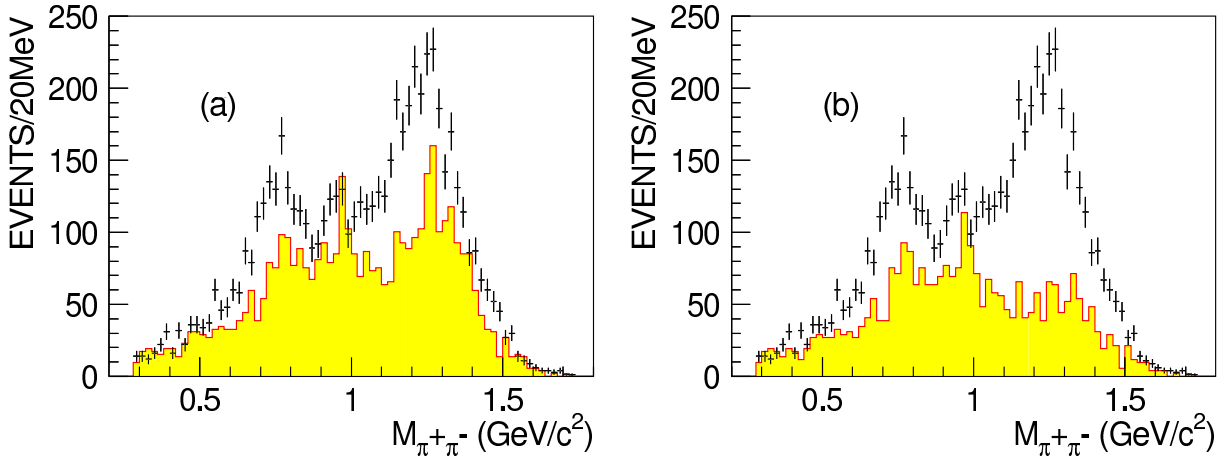


FIG. 2: The  $M_{\pi^+\pi^-}$  spectra from data and inclusive  $J/\psi$  decay Monte Carlo data, which are the sum of  $M_{\pi_1\pi_4}$  and  $M_{\pi_2\pi_3}$ . The dots with error bars are data, the shaded histogram is from inclusive  $J/\psi$  decay Monte Carlo data. (a) Including  $J/\psi \rightarrow f_2\rho^\pm\pi^\mp$ . (b)  $J/\psi \rightarrow f_2\rho^\pm\pi^\mp$  removed.

$J/\psi$  Monte Carlo decays is caused by  $J/\psi \rightarrow f_2\rho^\pm\pi^\mp$ .

Although  $J/\psi \rightarrow f_2\rho^\pm\pi^\mp$  decay is not listed in the PDG, we observe this decay in  $J/\psi \rightarrow \pi^0\pi^+\pi^-\pi^+\pi^-$ , and it gives a background in the  $M_{\pi^+\pi^-}$  spectrum of  $J/\psi \rightarrow \gamma f_2 f_2$ . There is an  $f_2$  signal in the  $M_{\pi^+\pi^-}$  distribution of  $J/\psi \rightarrow \pi^0\pi^+\pi^-\pi^+\pi^-$  when a  $\rho^\pm$  mass requirement is made on the other  $\pi^\pm\pi^0$  pair. The number of fitted  $f_2$  events in this  $M_{\pi^+\pi^-}$  distribution is 2111, and the efficiency, obtained by a Monte Carlo simulation, for this  $J/\psi \rightarrow f_2\rho^\pm\pi^\mp$  selection is 0.67%. The number of  $J/\psi \rightarrow f_2\rho^\pm\pi^\mp \rightarrow \pi^0\pi^+\pi^-\pi^+\pi^-$  events is  $N_{f_2\rho^\pm\pi^\mp} = 3.15 \times 10^5$ , which is used to determine the amount of  $f_2\rho^\pm\pi^\mp$  background in the  $M_{\pi^+\pi^-}$  spectrum of  $J/\psi \rightarrow \gamma f_2 f_2$ .

## V. RESULTS AND SYSTEMATIC ERRORS

The  $M_{\pi^+\pi^-}$  spectrum for events with  $M_{\pi^+\pi^-\pi^+\pi^-} \geq 2.6$  GeV and with one  $\pi^+\pi^-$  pair satisfying  $|M_{\pi^+\pi^-} - M_{f_2}| \leq 0.185$  GeV is used to obtain the number of  $J/\psi \rightarrow \gamma f_2 f_2$  events. The  $\pi^+\pi^-$  mass spectrum is fitted with a  $\rho^0$ , a  $f_2(1270)$ , and a 2nd order polynomial background plus  $f_2\rho^\pm\pi^\mp$  background using a binned maximum likelihood fit. The mass and width of the  $\rho^0$  are fixed at the PDG values. The shape of the  $f_2$  is determined by Monte Carlo simulation for  $J/\psi \rightarrow \gamma f_2 f_2$  ( $M_{f_2} = 1.275$  GeV,  $\Gamma_{f_2} = 0.185$  GeV). The shape of the  $f_2\rho^\pm\pi^\mp$  background is determined by Monte Carlo simulation of  $J/\psi \rightarrow f_2\rho^\pm\pi^\mp$  and normalized to the estimated number of  $J/\psi \rightarrow f_2\rho^\pm\pi^\mp$  background events. The fitting result is shown in Fig. 3. The  $M_{\pi^+\pi^-}$  spectrum is the sum of the  $M_{\pi^1\pi^4}$  and the  $M_{\pi^2\pi^3}$  spectra. The fitted number of  $f_2$  component in the  $M_{\pi^+\pi^-}$  spectrum is 1292 (both projections are used).

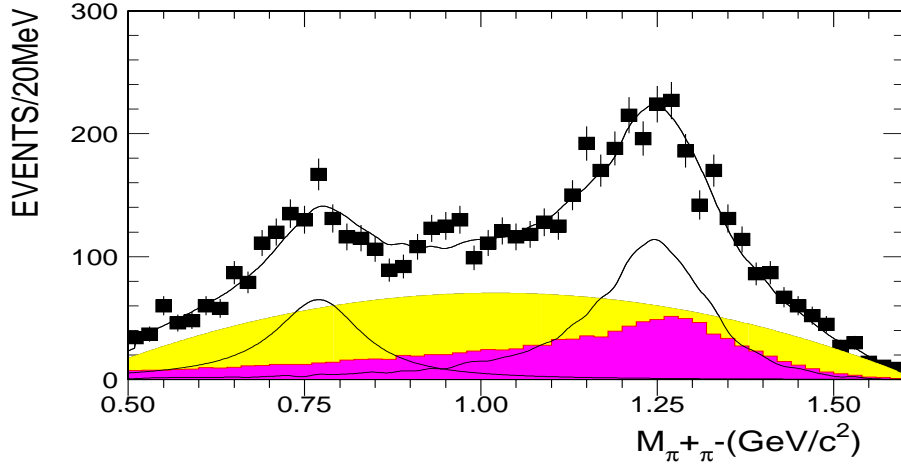


FIG. 3: Fit of the  $M_{\pi^+\pi^-}$  spectrum to obtain the  $f_2$  signal. The light shaded area is the 2nd order polynomial background. The dark shaded area is  $f_2\rho^\pm\pi^\mp$  background. The two peaks are  $\rho^0$  and  $f_2(1270)$ , respectively.

The branching ratio of  $J/\psi \rightarrow \gamma f_2 f_2$  can be determined with the following formula:

$$\begin{aligned} Br(J/\psi \rightarrow \gamma f_2 f_2) &= \frac{N^{obs}/\varepsilon}{N_{J/\psi} \cdot Br_{f_2 \rightarrow \pi^+\pi^-}^2} \\ &= (9.5 \pm 0.7) \times 10^{-4} \end{aligned}$$

where  $N^{obs} = 646 (= 1292/2)$  is the average number of survived  $J/\psi \rightarrow \gamma f_2 f_2$  events in  $M_{\pi^1\pi^4}$  projection and  $M_{\pi^2\pi^3}$  projection,  $\varepsilon = 3.71\%$  is the efficiency determined from phase space Monte Carlo events with the same cuts used to select  $J/\psi \rightarrow \gamma f_2 f_2$  data sample,  $N_{J/\psi} = 57.7 \times 10^6$  is the total number of  $J/\psi$  events collected by BESII [10], and  $Br_{f_2 \rightarrow \pi^+\pi^-} = 0.565$  is the branching ratio of  $f_2 \rightarrow \pi^+\pi^-$  [1].

TABLE I: Summary of systematic errors

Sources	Systematic error (%)
MDC tracking efficiency	8
PID efficiency	3
Photon selection	2
Kinematic fit	4
The number of $J/\psi$ events	4.7
$f_2$ width	5.1
$M_{\pi^+\pi^-\pi^+\pi^-}$ Cut	9.7
Background uncertainty	5.5
$Br_{f_2 \rightarrow \pi^+\pi^-}$	2.8
Total	16.5

Many sources of systematic errors are considered. Systematic errors associated with efficiencies, such as from the MDC tracking, particle identification, photon selection, and kinematic fitting, are determined by comparing  $\psi(2S)$  and  $J/\psi$  data with Monte Carlo simulation for very clean decay channels, such as  $\psi(2S) \rightarrow \pi^+\pi^- J/\psi$ .

The MDC tracking efficiency has been measured using channels like  $J/\psi \rightarrow \Lambda\bar{\Lambda}$  and  $\psi(2S) \rightarrow \pi^+\pi^- J/\psi$ ,  $J/\psi \rightarrow \mu^+\mu^+$ . It is found that the efficiency of the Monte Carlo simulation agrees with that of data within 1-2% per charged track. The total systematic error from the uncertainty of MDC tracking efficiency in our analysis is taken as 8%. The particle identification (PID) efficiency systematic error is calculated by comparing the efficiency of data with that of Monte Carlo. The largest difference between these two efficiencies is within 3%. According to the study of photon detection efficiency in  $J/\psi \rightarrow \rho\pi$  [11], SIMBES simulates the photon detection efficiency in the full energy range within 1 to 3%. Here, we take 2% as the systematic error in the photon detection efficiency.

The systematic error for the kinematic fit is caused by the differences between data and simulated data in the momenta and the error matrices of charged tracks and the energies and the directions of neutral tracks. To check the consistency between data and Monte Carlo simulation, two channels,  $J/\psi \rightarrow \rho^0\pi^0$  and  $J/\psi \rightarrow \Lambda\bar{\Lambda}$ , are analyzed for 2-prong and 4-prong events respectively. The systematic error for 4-prong events caused by kinematic fit is determined to be 4%.

Other sources of systematic errors come from the uncertainty of  $N_{J/\psi}$ , the  $f_2$  width, the  $M_{\pi^+\pi^-\pi^+\pi^-}$  requirement, and the uncertainty of the background. The total  $J/\psi$  number is  $(57.7 \pm 2.7) \times 10^6$  determined from 4-prong events [10]. The width of the  $f_2$  is  $185.1^{+3.4}_{-2.6}$  MeV [1]; 185.1 MeV is used in the Monte Carlo simulation. To estimate the systematic error caused by the width of  $f_2$ , 188.5 MeV and 182.5 MeV are also tried. After refitting the  $\pi^+\pi^-$  mass spectrum of Fig. 3, the relative differences of the branching ratios determined by using these two widths compared with the original one are 5.1% and -3.5% respectively. The systematic error caused by the  $f_2$  width is taken as 5.1%.

The requirement  $M_{\pi^+\pi^-\pi^+\pi^-} \geq 2.6$  GeV is used to select events for the determination of  $Br(J/\psi \rightarrow \gamma f_2 f_2)$ . The  $M_{\pi^+\pi^-\pi^+\pi^-}$  spectra of real data and Monte Carlo events are somewhat different. To estimate the systematic error caused by this requirement, we calculate  $Br(J/\psi \rightarrow \gamma f_2 f_2)$  with  $M_{\pi^+\pi^-\pi^+\pi^-} \geq 2.7$  GeV and compare the result with that obtained with  $M_{\pi^+\pi^-\pi^+\pi^-} \geq 2.6$  GeV. The relative difference is 9.7%, and this is taken as one of the systematic errors.

The background systematic error is caused by the uncertainty in the  $J/\psi \rightarrow f_2 \rho^\pm \pi^\mp$  background. This uncertainty is determined by varying the selection criteria used to obtain the number of  $J/\psi \rightarrow f_2 \rho^\pm \pi^\mp$  events. The systematic error caused by the uncertainty of  $J/\psi \rightarrow f_2 \rho^\pm \pi^\mp$  background is 5.5%.

Table I lists all the systematic errors, as well as the total systematic error of 16.5%, obtained by adding all contributions in quadrature. The branching ratio of  $J/\psi \rightarrow \gamma f_2(1270) f_2(1270)$  is

$$Br(J/\psi \rightarrow \gamma f_2(1270) f_2(1270)) = (9.5 \pm 0.7 \pm 1.6) \times 10^{-4},$$

where the first error is statistical and the second systematic. This branching ratio includes contributions from intermediate states such as  $J/\psi \rightarrow \gamma \eta_c$ .

## VI. SUMMARY

A new decay mode  $J/\psi \rightarrow \gamma f_2(1270) f_2(1270) \rightarrow \gamma \pi^+ \pi^- \pi^+ \pi^-$  is observed, and its branching ratio is measured to be  $Br(J/\psi \rightarrow \gamma f_2 f_2) = (9.5 \pm 0.7 \pm 1.6) \times 10^{-4}$ . This result will be helpful to understand the complex  $J/\psi \rightarrow \gamma \pi^+ \pi^- \pi^+ \pi^-$  decay.

## VII. ACKNOWLEDGMENT

The BES collaboration thanks the staff of BEPC for their hard efforts. This work is supported in part by the National Natural Science Foundation of China under contracts Nos. 19991480, 10225524, 10225525, the Chinese Academy of Sciences under contract No. KJ 95T-03, the 100 Talents Program of CAS under Contract Nos. U-11, U-24, U-25, and the Knowledge Innovation Project of CAS under Contract Nos. U-602, U-34 (IHEP); by the National Natural Science Foundation of China under Contract No. 10175060 (USTC), and No. 10225522 (Tsinghua University); and by the Department of Energy under Contract No. DE-FG03-94ER40833 (U Hawaii).

- 
- [1] S. Eidelman *et al.* (Particle Data Group), Phys. Letts. **B592**, 1 (2004).
  - [2] R. M. Baltrusaitis *et al.*, Phys. Rev. **D33**, 1222 (1986).
  - [3] J. Adler *et al.* (Mark-III Collaboration), SLAC-PUB-4686, *Submitted to 24th Int. Conf. on High Energy Physics, Munich, Germany, Aug 4-10, 1988.*
  - [4] D. Bisello *et al.*, Phys. Lett. **B200**, 215 (1988).
  - [5] J. Z. Bai *et al.* (BES Collaboration), Phys. Lett. **B472**, 207 (2000).
  - [6] J. Z. Bai *et al.* (BES Collaboration), Phys. Lett. **B555**, 174 (2003).
  - [7] J. Z. Bai *et al.* (BES Collaboration), Nucl. Instr. Meth. **A344**, 319 (1994).
  - [8] J. Z. Bai *et al.* (BES Collaboration), Nucl. Instr. Meth. **A458**, 627 (2001).
  - [9] J. C. Chen *et al.*, Phys. Rev. **D62**, 034003 (2000).
  - [10] S. S. Fang *et al.*, High Energy Phys. Nucl. Phys. **27**, 277 (2003) (in Chinese).
  - [11] S.M. Li *et al.*, High Energy Phys. Nucl. Phys. **28**, 64 (2004) (in Chinese).